Thermal and Residual Excited-State Population in a 3D Transmon Qubit

X. Y. Jin,[1,*] A. Kamal,[1] A. P. Sears,[2] T. Gudmundsen,[2] D. Hover,[2] J. Miloshi,[2] R. Slattery,[2] F. Yan,[1] J. Yoder,[2] T. P. Orlando,[1] S. Gustavsson,[1] and W. D. Oliver[1,2]

[1]*Research Laboratory of Electronics, Massachusetts Institute of Technology, 77 Massachusetts Avenue, Cambridge, Massachusetts 02139, USA*

[2]*MIT Lincoln Laboratory, 244 Wood Street, Lexington, Massachusetts 02420, USA*

(Received 30 November 2014; revised manuscript received 31 March 2015; published 15 June 2015)

Remarkable advancements in coherence and control fidelity have been achieved in recent years with cryogenic solid-state qubits. Nonetheless, thermalizing such devices to their milliKelvin environments has remained a long-standing fundamental and technical challenge. In this context, we present a systematic study of the first-excited-state population in a 3D transmon superconducting qubit mounted in a dilution refrigerator with a variable temperature. Using a modified version of the protocol developed by Geerlings *et al.*, we observe the excited-state population to be consistent with a Maxwell-Boltzmann distribution, *i.e.*, a qubit in thermal equilibrium with the refrigerator, over the temperature range 35–150 mK. Below 35 mK, the excited-state population saturates at approximately 0.1%. We verified this result using a flux qubit with ten times stronger coupling to its readout resonator. We conclude that these qubits have effective temperature $T_{\mathrm{eff}} = 35$ mK. Assuming T_{eff} is due solely to hot quasiparticles, the inferred qubit lifetime is 108 μs and in plausible agreement with the measured 80 μs.

DOI: 10.1103/PhysRevLett.114.240501 PACS numbers: 03.67.Lx, 85.25.Cp

Superconducting qubits are increasingly promising candidates to serve as the logic elements of a quantum information processor. This assertion reflects, in part, several successes over the past decade addressing the fundamental operability of this qubit modality [1–3]. A partial list includes a 5-orders-of-magnitude increase in the coherence time T_2 [4], the active initialization of qubits in their ground state [1,5], the demonstration of low-noise parametric amplifiers [6–12] enabling high-fidelity readout [13–16], and the implementation of a universal set of high-fidelity gates [17]. In addition, prototypical quantum algorithms [18–20] and simulations [21,22] have been demonstrated with few-qubit systems, and the basic parity measurements underlying certain error detection protocols are now being realized with qubit stabilizers [23–28] and photonic memories [29].

Concomitant with these advances is an enhanced ability to improve our understanding of the technical and fundamental limitations of single qubits. The 3D transmon [30] has played an important role in this regard, because its relatively clean electromagnetic environment, predominantly low-loss qubit-mode volume, and resulting long coherence times make it a sensitive test bed for probing these limitations.

One such potential limitation is the degree to which a superconducting qubit is in equilibrium with its cryogenic environment. Consider a typical superconducting qubit with a level splitting $E_{\mathrm{ge}} = hf_{\mathrm{ge}}$, with $f_{\mathrm{ge}} = 5$ GHz, mounted in a dilution refrigerator at temperature $T = 15$ mK, such that $E_{\mathrm{ge}} \gg k_{\mathrm{B}}T$. Ideally, such a qubit in thermal equilibrium with the refrigerator will have a thermal population $P_{|e\rangle} \approx 10^{-5}\%$ of its first excited state according to Maxwell-Boltzmann statistics. In practice, however, the empirical excited-state population reported for various superconducting qubits (featuring similar parameters E_{ge} and T) can be orders of magnitude higher, generally in the range of 1%–13% in the steady state, corresponding to effective temperatures $T_{\mathrm{eff}} = 50$–130 mK [1,31–33].

Thermalizing to milliKelvin temperatures has been a long-standing challenge for both normal and superconducting devices [34]. A primary cause is thermal noise or blackbody radiation from higher temperature stages driving the device out of equilibrium, e.g., via direct illumination or transferred via wires to the devices. Several techniques have been identified to reduce these effects, including the use of microwave dissipative filters [35] based on attenuation in meander lines [36,37], fine-grain powders [38–42], thin coaxial lines [42–44], and lossy transmission lines [45–47]; differential mode operation [48]; the importance of light-tight shielding practices [49]; and the introduction of low-reflectivity, infrared-absorbing ("black") surface treatments [50]. These techniques have been adapted to address the qubit excited-state population by reducing stray or guided thermal photons [31,51]. Nonetheless, the problem is not fully eliminated and, moreover, the mechanism that generates the residual excited-state population has yet to be clarified.

In this Letter, we report a systematic study of the excited-state population in a 3D transmon qubit as measured in our system. We developed a modified version of the protocol introduced by Geerlings *et al.* [1] to measure the

excited-state population $P_{|e\rangle}$ as a function of bath temperature. Our measurements are consistent with a qubit in thermal equilibrium with the dilution refrigerator over the temperature range 35–150 mK. For temperatures below 35 mK, $P_{|e\rangle}$ saturates to a residual value of approximately 0.1%, a factor 2.5 larger than the error of our measurement. Ascribing this residual population entirely to nonequilibrium hot quasiparticles, the upper limit of quasiparticle density is estimated to be 2.2×10^{-7} per Cooper pair. The corresponding quasiparticle-induced decay time is calculated to be $T_1 = 108\ \mu$s, in reasonable agreement with the independently measured decay time $T_1 = 80\ \mu$s. This suggests that both the residual excited-state population and relaxation times may be limited by quasiparticles for this device.

The experiments were conducted in a Leiden cryogen-free dilution refrigerator (model CF-450) with a base temperature of 15 mK. A temperature controller (model Lakeshore 370) is used to set the temperature with better than 0.1 mK stability at the thermometer. A detailed schematic indicating the placement and types of attenuation and filters used in this measurement is presented in the Supplemental Material [52].

The sample is a 5×5 mm^2 sapphire chip comprising an aluminum, single-junction 3D transmon qubit [30] with energy scales $E_J/E_C = 58$ and transition frequencies $f_{\mathrm{ge}} = 4.97$ GHz and $f_{\mathrm{ef}} = 4.70$ GHz. The qubit is controlled using a circuit-QED approach through its strong dispersive coupling ($g/2\pi = 160$ MHz) to an aluminum cavity with a TE101 mode frequency of 10.976 GHz (when loaded with a sapphire chip), an internal quality factor $Q_{\mathrm{i}} > 10^6$, and two ports with a net coupling $Q_{\mathrm{c}} = 10^5$. The chip is mounted in the geometric center of the cavity using indium at the corners. The sample in the present experiment exhibited coherence times: $T_1 = 80\ \mu$s (60–90 μs), $T_2^* = 115\ \mu$s (90–115 μs), and $T_{2E} = 154 \approx 2T_1\ \mu$s. The observed range of T_1 and T_2^* times over multiple cooldowns of this device are indicated parenthetically. All the experiments presented in this Letter are carried out with a standard dispersive readout method and without the use of a parametric amplifier.

In principle, when there is a nonzero excited-state population $P_{|e\rangle}$ in the qubit, one should be able to observe an $e \rightarrow f$ transition peak in qubit spectroscopy. In practice, however, it may be difficult to distinguish this transition experimentally from the background noise for small $P_{|e\rangle}$. In a recent publication [1], Geerlings *et al.* reported a method to measure small $P_{|e\rangle}$ levels ($\approx$1%–10%, $T_{\mathrm{eff}} = 60$–100 mK in their 3D transmon). In their approach, $P_{|e\rangle}$ is determined by driving a Rabi oscillation between qubit states $|e\rangle$ and $|f\rangle$, hereafter called an "e-f Rabi oscillation." In this work, we measured $P_{|e\rangle}$ using a modified protocol based on this method.

In Fig. 1(a), the readout-signal amplitude as a function of readout-signal frequency indicates the dressed cavity frequency for states $|g\rangle$, $|e\rangle$, and $|f\rangle$. For purposes of illustration, the qubit was prepared in state $|f\rangle$ using sequential $\pi^{\mathrm{g}\rightarrow\mathrm{e}}$ and $\pi^{\mathrm{e}\rightarrow\mathrm{f}}$ pulses, and then allowed to relax and partially populate states $|g\rangle$ and $|e\rangle$ before readout [56].

Whereas Geerlings *et al.* used a frequency corresponding to state $|g\rangle$ for qubit readout, in our experiment, we use the readout frequency corresponding to state $|e\rangle$ (red circle) to measure directly the e-f Rabi oscillation. Reading out state $|e\rangle$ simplifies the protocol by reducing the required number of $\pi^{\mathrm{g}\rightarrow\mathrm{e}}$ pulses. Moreover, since the readout tone for state $|e\rangle$ is off resonance with the cavity when the qubit is in state $|g\rangle$, its predominant state in this experiment, and the cavity Q is sufficiently high ($Q_c = 10^5$), the cavity is only resonantly excited during readout in the rare cases that the qubit is in state $|e\rangle$.

The modified measurement protocol is illustrated in Fig. 1(b). We measure the e-f Rabi oscillation for two different conditions. First, we apply a $\pi^{\mathrm{g}\rightarrow\mathrm{e}}$ pulse to the qubit, swapping the populations of states $|g\rangle$ and $|e\rangle$ [left panel, Fig. 1(b)]. We then apply an e-f driving pulse and read out state $|e\rangle$ as a function of the pulse duration. The resulting Rabi oscillation is measured for 1 μs, containing more than 4 periods, and it appears sinusoidal due to the long Rabi decay time $T_R > 100\ \mu$s. Note that the $\pi^{\mathrm{g}\rightarrow\mathrm{e}}$ pulse swaps the populations of state $|e\rangle$ and $|g\rangle$. Assuming the qubit population exists entirely within states $|g\rangle$, $|e\rangle$,

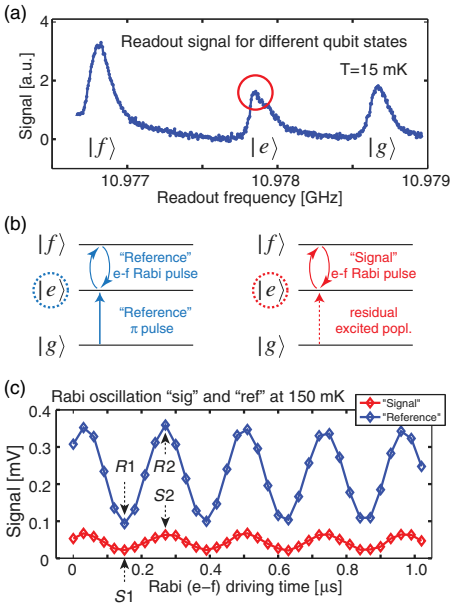

FIG. 1 (color online). (a) The readout signal versus readout frequency. Three well-separated peaks are visible, corresponding to different qubit states. We read out state $|e\rangle$. (b) Modified experiment protocol using e-f Rabi driving. The excited state is populated by a $\pi^{g\text{-}e}$ pulse (left panel) or environmental excitation (right panel). (c) Observed e-f Rabi oscillations at 150 mK. The blue trace determines A_{ref}, while the red trace determines A_{sig}. When A_{sig} is small, only two points on the blue trace ($R1$, $R2$) and the red trace ($S1$, $S2$) are measured. See text for details.

and $|f\rangle$, the oscillation amplitude is proportional to $P_{|g\rangle} - P_{|f\rangle}$, where $P_{|g\rangle}$ and $P_{|f\rangle}$ are the occupation probabilities of $|g\rangle$ and $|f\rangle$, respectively. We denote this amplitude A_{ref}, the reference used when determining $P_{|e\rangle}$.

Second, we solely apply an e-f Rabi driving pulse without the $\pi^{\mathrm{g}\to\mathrm{e}}$ pulse [right panel, Fig. 1(b)]. In this case, the observed oscillation amplitude is proportional to $P_{|e\rangle} - P_{|f\rangle}$. We denote the oscillation amplitude A_{sig}, the signal to be compared with the reference.

We are most interested in determining $P_{|e\rangle}$ in the low-temperature limit, *i.e.*, near the base temperature 15 mK. At sufficiently low bath temperatures, *i.e.*, $T \ll E_{\mathrm{ge}}/k_{\mathrm{B}} \approx E_{\mathrm{ef}}/k_{\mathrm{B}} \approx 235$ mK, we take $P_{|f\rangle} \to 0$ in our analytic treatment. This assumption is reasonable, since one normally expects $P_{|f\rangle} \le P_{|e\rangle} \le P_{|g\rangle}$ in the absence of extraneous coherent excitation (we observe no evidence of such excitations). Furthermore, simulated populations based on the Maxwell-Boltzmann distribution (see below) are consistent with this assumption for $T \le 50$ mK. It follows that $A_{\mathrm{sig}} = A_0 P_{|e\rangle}$ and $A_{\mathrm{ref}} = A_0 P_{|g\rangle}$, where A_0 is a factor converting the qubit state occupation probability to the readout voltage. In this limit, $P_{|e\rangle} + P_{|g\rangle} = 1$ and $A_{\mathrm{sig}} + A_{\mathrm{ref}} = A_0$, such that the population of state $|e\rangle$ is

$$P^{\mathrm{exp}}_{|e\rangle} \equiv A_{\mathrm{sig}}/A_0 = A_{\mathrm{sig}}/(A_{\mathrm{sig}} + A_{\mathrm{ref}}), \tag{1}$$

in which A_{sig} and A_{ref} are determined experimentally. We emphasize that for $T \le 50$ mK, $P^{\mathrm{exp}}_{|e\rangle}$ is a very good estimator for $P_{|e\rangle}$ in this device.

While measuring A_{ref} is straightforward due to its large signal-to-noise ratio, the main technical challenge is to measure A_{sig} precisely at the lowest temperatures. When the population of state $|e\rangle$ is in the range of 1%–10% [1], one can directly determine A_{sig} by fitting the observed e-f Rabi trace to a sinusoidal function. In our setup, a similarly discernable $P_{|e\rangle}$ level can be obtained by heating the sample to higher temperatures, where a thermally excited population at state $|e\rangle$ is significant. In Fig. 1(c), the e-f Rabi trace with (blue points) and without (red points) the $\pi^{g\to e}$ swap pulse were both visible at an elevated bath temperature of 150 mK, enabling us to measure directly both A_{ref} and A_{sig}.

In principle, provided one averages sufficiently, one can reduce the background noise and determine A_{sig} using this trace-fitting method. However, assuming that each experiment is independent, the background fluctuations decrease only as the square root of the number of trials averaged. Improving the resolution from 1% to 0.1% would require a factor 100× more trials and, thus, a factor 100× in time. As a result, for $P_{|e\rangle} \ll 1\%$, it is practically prohibitive to measure the entire trace in Fig. 1(c) (*i.e.*, 35 points, each requiring approximately 10^7 averages given our setup).

We therefore further modified the experimental protocol to increase data acquisition efficiency. Since we use the same e-f Rabi driving power to measure both the signal and the reference traces, we expect and confirmed the frequency and phase of these traces to be the same. We can therefore obtain amplitudes A_{sig} and A_{ref} by measuring two points each: the maximum $S1$ and minimum $S2$ amplitudes for the signal trace and, similarly, $R1$ and $R2$ for the reference trace [52]. Compared with measuring the full trace, this "two-point" method greatly reduces the acquisition time.

We designed a calibration experiment to validate the protocol. We first applied a small fraction of a $\pi^{\mathrm{g}\to\mathrm{e}}$ pulse to the qubit, which pumps $k\%$ of the ground-state population $P_{|g\rangle}$ to state $|e\rangle$, and simultaneously brings $k\%$ of any residual excited-state population $P_{|e\rangle}$ to ground state. The pumped excited-state population $P^p_{|e\rangle}$ is

$$P^p_{|e\rangle} = kP_{|g\rangle} + (1-k)P_{|e\rangle}, \tag{2}$$

in which $P_{|e\rangle}$ is the initial excited-state population. We then drove an e-f Rabi oscillation and measured the oscillation amplitude A_{sig}. The measured $P^p_{|e\rangle}$ should depend linearly on k, and its intercept at $k = 0$ (no pumping pulse) is $P_{|e\rangle}$ at base temperature (*i.e.*, assuming $P_{|f\rangle} = 0$).

We scanned k over the range 0.2%–5.0% and measured $P^p_{|e\rangle}$ at the base temperature $T = 15$ mK (see Fig. 2). The data fit well to a linear function, validating the protocol, and yield an intercept $P_{|e\rangle} = 0.067\%$, with 95% confidence bounds of (0.025%,0.011%). This value can, in fact, be regarded as one estimate for the residual excited-state population at the bath temperature of 15 mK.

When the bath temperature is raised, one expects that the excited-state population of the qubit will increase [see Fig. 1(c)] In thermal equilibrium with the refrigerator at temperature T, the qubit-state population of states $|i\rangle$ at energies E_i follow a Maxwell-Boltzmann distribution,

$$P_{|i\rangle} = \frac{1}{Z} g_i \exp(-E_i/k_B T). \tag{3}$$

Here, $Z = \sum_j g_j \exp(-E_j/k_B T)$ is the partition function, g_i is the degeneracy of each energy level E_i, and k_B is the Boltzmann constant. In our analysis, we define $E_{|g\rangle} \equiv 0$,

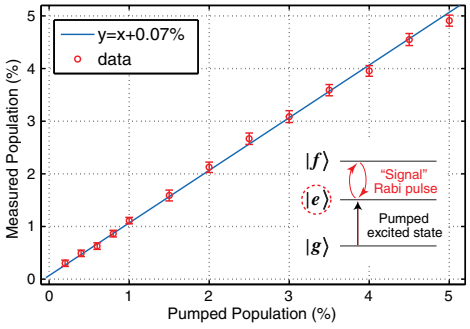

FIG. 2 (color online). Calibration measurement of excited state population (percent), pumped using a small fraction of a $\pi^{g\text{-}e}$ pulse. The data can be fit to a linear $y = x + b$ function, where $b = 0.067\%$, with 95% confidence bounds of (0.025%,0.011%).

$g_i = 1$, and consider the lowest-four energy levels in the transmon (a sufficient number for the temperature range considered here) [56]. Using Eq. (3), we calculate the equilibrium population $P_{|e\rangle}$ and the ratio $P^{\mathrm{exp}}_{|e\rangle}$ [see Eq. (1)] versus temperature, and plot them in Figs. 3(a) and 3(b). The equilibrium traces $P^{\mathrm{exp}}_{|e\rangle}$ and $P_{|e\rangle}$ are indistinguishable for $T \leq 50$ mK. At higher temperatures the assumption $P_{|f\rangle} = 0$ is no longer valid, and the traces differ by as much as 2% at 160 mK.

Excited-state population measurements were performed as a function of temperature over the range $T = 15$–150 mK. For each set point, after the temperature sensor (fixed on the cold finger near the device) reading is stable to within 0.1 mK, we wait an additional 2 h before acquiring data to ensure the qubit has reached its steady-state population distribution. In Fig. 3(a) the experimental $P^{\mathrm{exp}}_{|e\rangle}$ generally matches the simulation of Eq. (1) assuming Maxwell-Boltzmann populations (black trace) over the range 35–150 mK, consistent with the qubit being in thermal equilibrium with the cryostat. In the range 35–60 mK, $P^{\mathrm{exp}}_{|e\rangle}$ also matches the Maxwell-Boltzmann estimate for $P_{|e\rangle}$ (red trace). Below 35 mK [Fig. 3(b)], the experimental $P^{\mathrm{exp}}_{|e\rangle}$ deviates from thermal equilibrium, saturating at approximately $P^{\mathrm{exp}}_{|e\rangle} = P_{|e\rangle} = 0.1\%$ (purple dashed line). That is, $P^{\mathrm{exp}}_{|e\rangle} \leq 0.1\% + P_{|f\rangle}$ and becomes

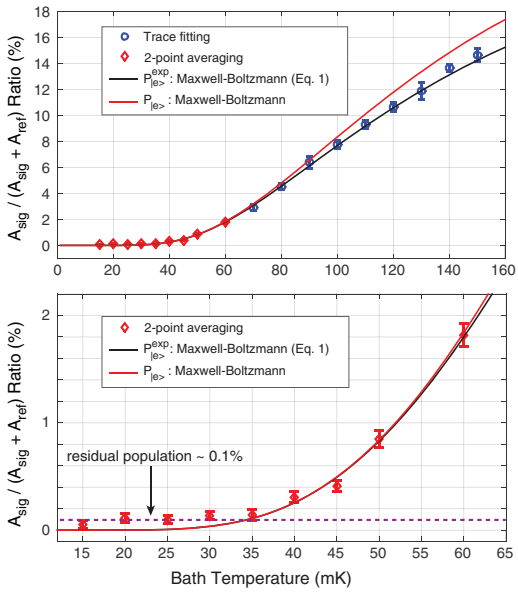

FIG. 3 (color online). (a) $P^{\mathrm{exp}}_{|e\rangle}$ ratio [Eq. (1)] versus temperature, 15–150 mK. Experimental data are obtained through fitting a 1-μs Rabi trace (blue points) or the two-point method (red points). Solid lines are calculated $P^{\mathrm{exp}}_{|e\rangle}$ (blue line) and $P_{|e\rangle}$ (red line) based on the Maxwell-Boltzmann distribution for the lowest four energy levels (see text). (b) Zoom: $P^{\mathrm{exp}}_{|e\rangle}$ ratio versus temperature, 15–60 mK. In this limit, $P^{\mathrm{exp}}_{|e\rangle}$ is a good estimator for $P_{|e\rangle}$ The data saturate to 0.1% at lower temperatures (purple dashed line) with an inferred effective temperature of 35 mK.

$P^{\mathrm{exp}}_{|e\rangle} = 0.1\%$ with the reasonable assumption $P_{|f\rangle} = 0$ [see Eq. (1)]. This saturation level is consistent with the 0.067% estimate obtained during the calibration experiment (Fig. 2). Although $P_{|e\rangle} = 0.1\%$ is an order of magnitude lower than other reports in the literature, it remains about 4 orders of magnitude higher than the expected equilibrium value ($\sim 10^{-5}\%$) at 15 mK. We note that we used a level of averaging sufficient to achieve small (0.04%) error bars on the population of 0.1%. In addition to more averaging, using a low-noise parametric amplifier would further improve the signal-to-noise ratio and allow for single-shot readout with higher resilience to low-frequency noise [52].

We define an effective temperature T_{eff} as the temperature that would have generated the observed $P_{|e\rangle}$ in an otherwise identical equilibrium qubit, according to Eq. (3). In our qubit, the crossover from thermal equilibrium to saturation at $P_{|e\rangle} = 0.1\%$ occurs at $T_{\mathrm{eff}} = 35$ mK.

A potential mechanism for the observed nonequilibrium qubit temperature is the presence of "hot" nonequilibrium quasiparticles (*i.e.*, those with energy higher than $\Delta + E_{\mathrm{ge}}$, where Δ is the superconducting energy gap) [57]. Stray thermal photons entering the cavity from higher-temperature stages of the refrigerator may in principle generate new quasiparticles or heat existing ones depending on the photon energy. Such "hot" quasiparticles, in turn, lose energy E_{ge} to the qubit and drive it out of thermal equilibrium to a degree determined by the nonequilibrium quasiparticle density. Following Wenner *et al.*, the quasiparticle-induced excited-state population can be written as [57]

$$P^{\mathrm{qp}}_{|e\rangle} \simeq 2.17(n_{\mathrm{qp}}/n_{\mathrm{cp}})(\Delta/E_{\mathrm{ge}})^{3.65}, \tag{4}$$

in which n_{cp} is the Cooper-pair density and n_{qp} is the density of all quasiparticles. Taking the observed excited-state population $P^{\mathrm{qp}}_{|e\rangle} = 0.1\%$ to be solely induced by quasiparticles, the upper limit for the quasiparticle density is $(n_{\mathrm{qp}}/n_{\mathrm{cp}}) = 2.2 \times 10^{-7}$ per Cooper pair.

Within these assumptions, the quasiparticle-induced decay rate for a transmon qubit is [57,58]

$$\Gamma_{\mathrm{qp}} \simeq \frac{\sqrt{2}}{R_N C}\left(\frac{\Delta}{E_{\mathrm{ge}}}\right)^{3/2}\frac{n_{\mathrm{qp}}}{n_{\mathrm{cp}}}, \tag{5}$$

in which R_N is the normal-state resistance of the Josephson junction, and C is the qubit capacitance. Taking $\Delta = 170$ μeV, $R_N = 9.5$ kΩ and $C = 80$ fF [52,56], we have $\Gamma_{\mathrm{qp}} = 9.30$ kHz, corresponding to a relaxation time $T_1^{\mathrm{qp}} = 108$ μs, which is only about 35% larger than the measured time $T_1 = 80$ μs for this sample.

We have measured similar effective temperatures $T_{\mathrm{eff}} =$ 30–45 mK for several superconducting qubit modalities (flux qubit, capacitively shunted flux qubit, 2D transmons) measured in our lab in both a dry (Leiden CF-450) and a

wet (Oxford Kelvinox 400) refrigerator with similar wiring and filtering configurations [52]. In particular, we observed $T = 35 \pm 4$ mK for a capacitively shunted flux qubit with similar qubit parameters, including $f_{ge} = 4.7$ GHz, $f_{resonator} = 8.3$ GHz, $Q_c = 5000$ and $g/2\pi = 100$ MHz. This is notable, because this device was read out dispersively using a cavity with 10× lower Q_c, that is, with a much stronger coupling to the coaxial cables in our refrigerator than the 3D transmon.

To summarize, we have studied the first-excited-state population of a 3D transmon qubit over the temperature range $T = 15$–150 mK. The excited-state population matches Maxwell-Boltzmann statistics over the range $T = 35$–150 mK, consistent with a qubit in thermal equilibrium with the refrigerator. For temperatures below 35 mK, the excited-state population saturates to a small value of approximately 0.1%. Assuming the residual population is solely caused by nonequilibrium hot quasiparticles, the calculated and measured relaxation times are plausibly consistent for this device. We have observed similarly low effective temperature in multiple devices and configurations, including a readout resonator with 10× larger coupling Q. While we present our full filtering and attenuation schematic in the Supplemental Material [52], we did not need to change any particular aspect of our measurement system to achieve these effective temperatures, and so there is no particular "reason" beyond careful cryogenic engineering that we can identify for their relatively low values.

We thank George Fitch and Terry Weir for technical assistance and A. J. Kerman for useful discussions. This research was funded in part by the Assistant Secretary of Defense for Research & Engineering and by the Office of the Director of National Intelligence (ODNI), Intelligence Advanced Research Projects Activity (IARPA) via MIT Lincoln Laboratory under Air Force Contract No. FA8721-05-C-0002; by the U.S. Army Research Office Grant No. W911NF-14-1-0078; and by the National Science Foundation Grant No. PHY-1415514. The views and conclusions contained herein are those of the authors and should not be interpreted as necessarily representing the official policies or endorsements, either expressed or implied, of ODNI, IARPA, or the US Government.

*jin@mit.edu

[1] K. Geerlings, Z. Leghtas, I. M. Pop, S. Shankar, L. Frunzio, R. J. Schoelkopf, M. Mirrahimi, and M. H. Devoret, Demonstrating a driven reset protocol for a superconducting qubit., Phys. Rev. Lett. **110**, 120501 (2013).

[2] D. P. DiVincenzo, The physical implementation of quantum computation., arXiv:quant-ph/0002077v3.

[3] M. H. Devoret and R. J. Schoelkopf, Superconducting circuits for quantum information: An outlook., Science **339**, 1169 (2013).

[4] W. D. Oliver and P. B. Welander, Materials in superconducting quantum bits., MRS Bull. **38**, 816 (2013).

[5] S. O. Valenzuela, W. D. Oliver, D. M. Berns, K. K. Berggren, L. S. Levitov, and T. P. Orlando, Microwave-induced cooling of a superconducting qubit., Science **314**, 1589 (2006).

[6] M. A. Castellanos-Beltran and K. W. Lehnert, Widely tunable parametric amplifier based on a superconducting quantum interference device array resonator., Appl. Phys. Lett. **91**, 083509 (2007).

[7] T. Yamamoto, K. Inomata, M. Watanabe, K. Matsuba, T. Miyazaki, W. D. Oliver, Y. Nakamura, and J. Tsai, Flux-driven Josephson parametric amplifier., Appl. Phys. Lett. **93**, 042510 (2008).

[8] N. Bergeal, F. Schackert, M. Metcalfe, R. Vijay, V. E. Manucharyan, L. Frunzio, D. E. Prober, R. J. Schoelkopf, S. M. Girvin, and M. H. Devoret, Phase-preserving amplification near the quantum limit with a Josephson ring modulator., Nature (London) **465**, 64 (2010).

[9] M. Hatridge, R. Vijay, D. H. Slichter, J. Clarke, and I. Siddiqi, Dispersive magnetometry with a quantum limited squid parametric amplifier., Phys. Rev. B **83**, 134501 (2011).

[10] K. M. Sundqvist, S. Kintaş, M. Simoen, P. Krantz, M. Sandberg, C. M. Wilson, and P. Delsing, The pumpistor: A linearized model of a flux-pumped superconducting quantum interference device for use as a negative-resistance parametric amplifier., Appl. Phys. Lett. **103**, 102603 (2013).

[11] J. Y. Mutus, T. C. White, E. Jeffrey, D. Sank, R. Barends, J. Bochmann, Y. Chen, Z. Chen, B. Chiaro, A. Dunsworth *et al.*, Design and characterization of a lumped element single-ended superconducting microwave parametric amplifier with on-chip flux bias line., Appl. Phys. Lett. **103**, 122602 (2013).

[12] K. O'Brien, C. Macklin, I. Siddiqi, and X. Zhang, Resonantly phase-matched Josephson junction traveling wave parametric amplifier., Phys. Rev. Lett. **113**, 157001 (2014).

[13] R. Vijay, D. H. Slichter, and I. Siddiqi, Observation of quantum jumps in a superconducting artificial atom., Phys. Rev. Lett. **106**, 110502 (2011).

[14] G. de Lange, D. Ristè, M. Tiggelman, C. Eichler, L. Tornberg, G. Johansson, A. Wallraff, R. Schouten, and L. DiCarlo, Reversing quantum trajectories with analog feedback., Phys. Rev. Lett. **112**, 080501 (2014).

[15] Z. R. Lin, K. Inomata, W. D. Oliver, K. Koshino, Y. Nakamura, J. S. Tsai, and T. Yamamoto, Single-shot readout of a superconducting flux qubit with a flux-driven Josephson parametric amplifier., Appl. Phys. Lett. **103**, 132602 (2013).

[16] B. Abdo, K. Sliwa, S. Shankar, M. Hatridge, L. Frunzio, R. Schoelkopf, and M. Devoret, Josephson directional amplifier for quantum measurement of superconducting circuits., Phys. Rev. Lett. **112**, 167701 (2014).

[17] R. Barends, J. Kelly, A. Megrant, A. Veitia, D. Sank, E. Jeffrey, T. C. White, J. Mutus, A. G. Fowler, B. Campbell *et al.*, Superconducting quantum circuits at the surface code threshold for fault tolerance., Nature (London) **508**, 500 (2014).

[18] L. DiCarlo, J. M. Chow, J. M. Gambetta, L. S. Bishop, B. R. Johnson, D. I. Schuster, J. Majer, A. Blais, L. Frunzio, S. M. Girvin *et al.*, Demonstration of two-qubit algorithms with a superconducting quantum processor., Nature (London) **460**, 240 (2009).

[19] M. D. Reed, L. DiCarlo, S. E. Nigg, L. Sun, L. Frunzio, S. M. Girvin, and R. J. Schoelkopf, Realization of three-qubit quantum error correction with superconducting circuits., Nature (London) **482**, 382 (2012).
[20] E. Lucero, R. Barends, Y. Chen, J. Kelly, M. Mariantoni, A. Megrant, P. OMalley, D. Sank, A. Vainsencher, J. Wenner *et al.*, Computing prime factors with a Josephson phase qubit quantum processor., Nat. Phys. **8**, 719 (2012).
[21] S. Gustavsson, J. Bylander, and W. D. Oliver, Time-reversal symmetry and universal conductance fluctuations in a driven two-level system., Phys. Rev. Lett. **110**, 016603 (2013).
[22] Y. Chen, P. Roushan, D. Sank, C. Neill, E. Lucero *et al.*, Emulating weak localization using a solid-state quantum circuit., Nat. Commun. **5**, 5184 (2014).
[23] D. Ristè, M. Dukalski, C. A. Watson, G. de Lange, M. J. Tiggelman, Y. M. Blanter, K. W. Lehnert, R. N. Schouten, and L. DiCarlo, Deterministic entanglement of superconducting qubits by parity measurement and feedback., Nature (London) **502**, 350 (2013).
[24] O.-P. Saira, J. P. Groen, J. Cramer, M. Meretska, G. de Lange, and L. DiCarlo, Entanglement genesis by ancilla-based parity measurement in 2d circuit qed., Phys. Rev. Lett. **112**, 070502 (2014).
[25] J. M. Chow, J. M. Gambetta, E. Magesan, S. J. Srinivasan, A. W. Cross, D. W. Abraham, N. A. Masluk, B. Johnson, C. A. Ryan, and M. Steffen, Implementing a strand of a scalable fault-tolerant quantum computing fabric., Nat. Commun. **5**, 4015 (2014).
[26] J. Kelly *et al.*, State preservation by repetitive error detection in a superconducting quantum circuit., Nature (London) **519**, 66 (2015).
[27] A. Córcoles, E. Magesan, S. J. Srinivasan, A. W. Cross, M. Steffen, J. M. Gambetta, and J. M. Chow, Detecting arbitrary quantum errors via stabilizer measurements on a sublattice of the surface code., arXiv:1410.6419.
[28] D. Ristè, S. Poletto, M.-Z. Huang, A. Bruno, V. Vesterinen, O.-P. Saira, and L. DiCarlo, Detecting bit-flip errors in a logical qubit using stabilizer measurements., Nat. Commun. **6**, 6983 (2015).
[29] L. Sun, A. Petrenko, Z. Leghtas, B. Vlastakis, G. Kirchmair, K. M. Sliwa, A. Narla, M. Hatridge, S. Shankar, J. Blumoff *et al.*, Tracking photon jumps with repeated quantum non-demolition parity measurements., Nature (London) **511**, 444 (2014).
[30] H. Paik, D. I. Schuster, L. S. Bishop, G. Kirchmair, G. Catelani, A. P. Sears, B. R. Johnson, M. J. Reagor, L. Funzio, L. I. Glazman, S. M. Girvin, M. H. Devoret, and R. J. Schoelkopf, Observation of high coherence in Josephson junction qubits measured in a three-dimensional circuit qed architecture., Phys. Rev. Lett. **107**, 240501 (2011).
[31] A. D. Corcoles, J. M. Chow, J. M. Gambetta, C. Rigetti, J. Rozen, G. A. Keefe, M. B. Rothwell, M. B. Ketchen, and M. Steffen, Protecting superconducting qubits from radiation., Appl. Phys. Lett. **99**, 181906 (2011).
[32] J. E. Johnson, C. Macklin, D. H. Slichter, R. Vijay, E. B. Weingarten, J. Clarke, and I. Siddiqi, Heralded state preparation in a superconducting qubit., Phys. Rev. Lett. **109**, 050506 (2012).
[33] D. Ristè, C. C. Bultink, K. W. Lehnert, and L. DiCarlo, Feedback control of a solid-state qubit using high-fidelity projective measurement., Phys. Rev. Lett. **109**, 240502 (2012).
[34] F. Giazotto, T. T. Heikkilä, A. Luukanen, A. M. Savin, and J. P. Pekola, Opportunities for mesoscopics in thermometry and refrigeration: Physics and applications., Rev. Mod. Phys. **78**, 217 (2006).
[35] K. Bladh, D. Gunnarsson, E. Hürfeld, S. Devi, C. Kristoffersson, B. Smålander, S. Pehrson, T. Cleason, P. Delsing, and M. Taslakov, Comparison of cryogenic filters for use in single electronics experiments., Rev. Sci. Instrum. **74**, 1323 (2003).
[36] D. Vion, P. F. Orfila, P. Joyez, D. Esteve, and M. H. Devoret, Miniature electrical filters for single electron devices., J. Appl. Phys. **77**, 2519 (1995).
[37] H. le Sueur and P. Joyez, Microfabricated electromagnetic filters for millikelvin experiments., Rev. Sci. Instrum. **77**, 115102 (2006).
[38] M. H. Devoret, J. Martinis, and J. Clarke, Measurements of macroscopic quantum tunneling out of the zero-voltage state of a current-biased josephson junction., Phys. Rev. Lett. **55**, 1908 (1985).
[39] J. Martinis, M. H. Devoret, and J. Clarke, Experimental tests for the quantum behavior of a macroscopic degree of freedom: The phase difference across a Josephson junction., Phys. Rev. B **35**, 4682 (1987).
[40] F. P. Milliken, J. R. Rozen, G. A. Keefe, and R. H. Koch, 50Ω characteristic impedance low-pass metal powder filters., Rev. Sci. Instrum. **78**, 024701 (2007).
[41] A. Lukashenko and A. Ustinov, Improved powder filters for qubit measurements., Rev. Sci. Instrum. **79**, 014701 (2008).
[42] A. Fukushima, A. Sato, A. Iwasa, Y. Nakamura, Y. Komatsuzaki, and Y. Sakamoto, Attenuation of microwave filters for single-electron tunneling experiments., IEEE Trans. Instrum. Meas. **46**, 289 (1997).
[43] A. B. Zorin, The thermocoax cable as the microwave frequency filter for single electron circuits., Rev. Sci. Instrum. **66**, 4296 (1995).
[44] D. C. Glattli, P. Jacques, A. Kumar, P. Pari, and L. Saminadayar, A noise detection scheme with 10 mk noise tempearture resolution for semiconductor single electron tunneling devices., J. Appl. Phys. **81**, 7350 (1997).
[45] H. Courtois, O. Buisson, J. Chaussy, and B. Pannetier, Miniature low-temperature high-frequency filters for single electronics., Rev. Sci. Instrum. **66**, 3465 (1995).
[46] D. F. Santavicca and D. E. Prober, Impedance-matched low-pass stripline filters., Meas. Sci. Technol. **19**, 087001 (2008).
[47] D. H. Slichter, O. Naaman, and I. Siddiqi, Millikelvin thermal and electrical performance of lossy transmission line filters., Appl. Phys. Lett. **94**, 192508 (2009).
[48] R. Vijay, M. H. Devoret, and I. Siddiqi, Invited review article: The josephson bifurcation amplifier., Rev. Sci. Instrum. **80**, 111101 (2009).
[49] J. M. Hergenrother, J. G. Lu, M. T. Tuominen, D. C. Ralph, and M. Tinkham, Photon-activated switch ehavior in the single-electron transistor with a superconducting island., Phys. Rev. B **51**, 9407 (1995).

[50] M. Persky, Review of black surfaces for space-borne infrared systems., Rev. Sci. Instrum. **70**, 2193 (1999).

[51] R. Barends, J. Wenner, M. Lenander, Y. Chen, R. C. Bialczak, J. Kelly, E. Lucero, P. OMalley, M. Mariantoni, D. Sank *et al.*, Minimizing quasiparticle generation from stray infrared light in superconducting quantum circuits., Appl. Phys. Lett. **99**, 113507 (2011).

[52] See Supplemental Material at http://link.aps.org/supplemental/10.1103/PhysRevLett.114.240501, for experimental setup and measurement protocols in detail, which includes Refs. [53–55].

[53] F. Yan, S. Gustavsson, A. Kamal, J. Birenbaum, A. P. Sears, D. Hover, T. J. Gudmundsen, J. L. Yoder, T. P. Orlando, J. Clarke, A. J. Kerman, and W. D. Oliver, (to be published).

[54] V. Ambegaokar and A. Baratoff, Tunneling Between Superconductors, Phys. Rev. Lett. **10**, 486(E) (1963).

[55] V. Ambegaokar and A. Baratoff, Tunneling Between Superconductors, Phys. Rev. Lett. **11**, 104 (1963).

[56] M. J. Peterer, S. J. Bader, X. Jin, F. Yan, A. Kamal, T. J. Gudmundsen, P. J. Leek, T. P. Orlando, W. D. Oliver, and S. Gustavsson, Coherence and decay of higher energy levels of a superconducting transmon qubit., Phys. Rev. Lett. **114**, 010501 (2015).

[57] J. Wenner, Y. Yin, E. Lucero, R. Barends, Y. Chen, B. Chiaro, J. Kelly, M. Lenander, M. Mariantoni, A. Megrant, C. Neill, P. J. J. O'Malley, D. Sank, A. Vainsencher, H. Wang, T. C. White, A. N. Cleland, and J. M. Martinis, Excitation of superconducting qubits from hot nonequilibrium quasiparticles., Phys. Rev. Lett. **110**, 150502 (2013).

[58] G. Catelani, J. Koch, L. Frunzio, R. Schoelkopf, M. Devoret, and L. Glazman, Quasiparticle relaxation of superconducting qubits in the presence of flux., Phys. Rev. Lett. **106**, 077002 (2011).